

A Framework for Incorporation of Infeed Uncertainty in Power System Risk-Based Security Assessment

Martijn de Jong^{ID}, Georgios Papaefthymiou, *Member, IEEE*, and Peter Palensky, *Senior Member, IEEE*

Abstract—In this paper, a risk-based security assessment methodology is presented, which allows the assessment of operational security of a power system's future state under uncertainty deriving from varying topology scenarios (contingencies) and forecast errors (loads and renewable infeeds). The methodology models input uncertainty with a copula function-based Monte-Carlo (MC) framework. Furthermore, it provides the highest level of accuracy on initiating causes of failures through an AC power flow (AC PF) framework. Finally, it achieves speed in solution by the combination of two measures of risk. A fast screening tool, based on severity functions, allows us to quickly screen the system for the most severe states. A detailed analysis tool, based on an AC optimal power flow (AC OPF) framework and the notion of lost load, provides additional valuable information, including remedial actions to steer away from severe system states. This paper presents results from the application of the methodology proving the necessity of such a framework. It is shown that not taking into account stochastic dependence through a proper MC setup seriously underestimates system risk and that an AC framework is needed, as voltage deviations are shown to often be initiators of system collapse.

Index Terms—AC OPF, copula theory, correlation, RBSA, Monte-Carlo simulation, severity functions, stochastic dependence.

I. INTRODUCTION

IN RECENT years, power systems undergo radical changes in the way they are planned and operated, with detrimental effects on the system operational risk. On the one hand, the shift from a regulated monopoly to a competitive market framework reduces the ability of system operators to plan and control conventional units, reducing the overall system controllability. On the other hand, the system infeeds become highly uncertain, due to the increased share of stochastic renewable energy sources (RES) and due to the changes in power demand by the

Manuscript received September 16, 2016; revised January 12, 2017; accepted March 11, 2017. Date of publication March 27, 2017; date of current version December 20, 2017. This work was supported by the FP-7 Umbrella project under Grant 282775. Paper no. TPWRS-01391-2016. (*Corresponding author:* Martijn de Jong.)

M. de Jong is with the Delft Institute of Applied Mathematics, Delft University of Technology, 2628 CD Delft, The Netherlands (e-mail: m.a.dejong-2@tudelft.nl).

G. Papaefthymiou is with the Department of Electrical Sustainable Energy, Delft University of Technology, 2628 CD Delft, The Netherlands, and also with Elia Grid International GmbH, 10557 Berlin, Germany (e-mail: g.papaefthymiou@tudelft.nl).

P. Palensky is with the Department of Electrical Sustainable Energy, Delft University of Technology, 2628 CD Delft, The Netherlands (e-mail: P.Palensky@tudelft.nl).

Color versions of one or more of the figures in this paper are available online at <http://ieeexplore.ieee.org>.

Digital Object Identifier 10.1109/TPWRS.2017.2687983

electrification of the transport (electric mobility) and heat sectors (heat pumps in buildings) [1]. Safeguarding the reliability of the power system is a key enabler for this massive system transformation. For the operation of future power systems, new methods are needed to incorporate the different sources of uncertainty (contingencies, load and RES forecast errors) during the operational planning stage (day- to hour- ahead) and to help system operators to steer the system into risk-averse modes of operation [2]–[4].

In this regard, valuable research has been conducted to develop tools for transmission system operators (TSOs) to monitor and control the power system and its security. In this paper security is defined as (i) the ability of the power system to withstand sudden disturbances such as unanticipated loss of system elements [5], and (ii) disturbances caused by uncertainty in load and generation profiles due to forecast errors.

A first stream of research is the usage of so-called severity functions in RBSA. In [6] and [7] an approach for online RBSA is proposed based on risk indices, one for each of the following problems: too low voltage, circuit overloading, voltage instability and cascading. The risk index is defined to be the expectation of severity, where, for a certain system state, the severity is computed using appropriate severity functions. A pre-defined list of most probable contingencies is used in the methodology and cascading events are modeled with a looping mechanism based on hard limits on the maximum allowable power flow through the circuits. The concept of severity functions has since then widely been used: recently, in [8] severity functions are used to investigate transmission line overloading in power systems with wind and load-power generation correlation, and in [9] severity functions are used in a contingency ranking method.

A second stream of research is the usage of a MC framework in power system risk assessment with as a risk indicator lost load or expected energy not served (EENS). In [2], [10] and [11] a methodology based on MC sampling is advocated to adequately capture stochasticity and assessing risk in power system operation, focusing on the complex behaviour of random disturbances resulting from cascading, sympathetic tripping, weather effects and hidden failures. Both streams highlight the importance of use of full AC PF information in order to properly capture the initiating causes of failures (circuit overloads and voltage problems).

A third stream of research has focused on the analysis of spatiotemporal dependencies of system RES infeeds, in particular pointing out to two key properties: the non-Gaussianity of marginal distributions and the complex dependence structures.

A series of papers was published [12]–[16] proposing MC using copula functions as the most appropriate modeling framework for such type of uncertainty. As shown in [13], [17], [18], using methods that do not properly model stochastic dependence can lead to a severe underestimation of the system risk. In [16], the framework was extended to the simulation of probabilistic forecasts, capturing spatiotemporal interdependencies in prediction errors. In [19], the framework was further extended to include other copula functions (Archimedian and elliptical copulas) for modeling wind power uncertainty.

For these reasons, RBSA methods to assess systems with high shares of RES, must meet the following three key conditions:

- 1) can properly capture input forecast uncertainty (loads/RES): the complex stochasticity necessitates taking into account stochastic dependence between variables.
- 2) can use detailed power flow information in terms of full AC PF computations to capture
 - a) circuit overloading and;
 - b) voltage violations.
- 3) can achieve this level of accuracy with computational speed that allows for close-to-real-time applications.

In this paper a methodology is presented which meets the three key conditions by combining features from the aforementioned streams of research. The methodology:

- 1) utilizes a MC framework with copulas to capture input uncertainty;
- 2) provides the highest level of accuracy on initiating causes of failures through a combination of AC PF and AC OPF;
- 3) Achieves speed in solution by combining
 - a) a fast system risk screening tool that estimates the risk level based on severity functions with;
 - b) a detailed analysis tool that zooms in the risk regions and assesses remedial actions in order to steer the system in risk-averse mode;
 - c) a dynamic MC sampling method that allows changing the number of samples for each risk zone based on the needed accuracy.

The application of severity functions is used for the screening tool. These functions allow to quickly screen the system for (the most) severe system states. Moreover, a mechanism based on hard limits is used to capture cascading overloads. A methodology is followed based on MC sampling and the computation of lost load as basis for the detailed analysis tool. The required remedial actions and the amount of lost load are computed by solving an AC OPF problem. The AC OPF framework provides a flexible environment to assess a large set of remedial actions, including the usage of power flow controlling components (PFCCs), re-dispatching actions or topology optimization. Furthermore, in our methodology MC sampling in combination with the copula theory is used in order to be able to adequately capture the complex stochasticity of wind and solar forecast errors. In this paper contingencies¹ are not considered; however, the methodology can easily be extended for contingency screening as well.

¹A contingency is an unexpected failure or outage of a network component, e.g., a generator, transmission line or transformer [5]. In operational planning, a set of critical contingencies are chosen in order to reduce calculation time for system security assessment.

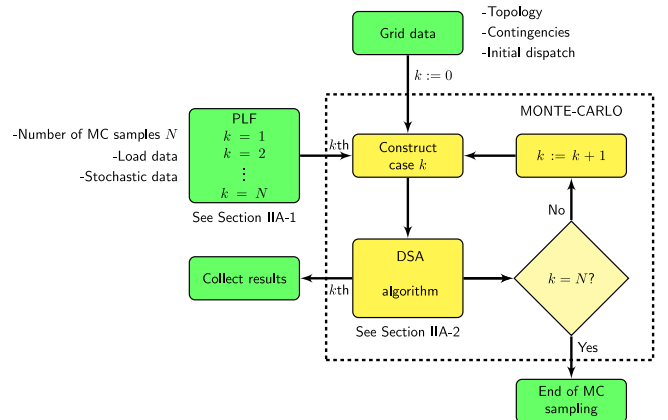


Fig. 1. Overview of methodology: MC framework with DSA as core and key inputs/outputs (green colour).

The paper is organized as follows. In Section II the methodology is presented, explaining the implementation of both risk metrics in a stochastic AC PF framework. In Section II-A an overview of the methodology is provided. In Section II-B the concept of severity functions is explained which is the key concept in Tool I, the screening tool. In Section II-C Tool II, the detailed analysis tool, is presented. In Section III the experimental setup for a case study on the IEEE 118 bus test system is presented. The case studies and accompanying results are presented and discussed in Section IV. Conclusions can be found in Section V.

II. PROPOSED METHODOLOGY

A. Overview

The methodology combines a MC framework with a detailed deterministic security assessment algorithm, see Fig. 1.

1) Sample Generation: As the presented methodology is modular, basically any sample generation method can be used to generate a probabilistic load flow (PLF). Here a copula-function based MC framework is used for the sampling of the system inputs. This method is very proficient to capture the complex stochasticity of the system inputs, namely modeling of any type of marginal distributions, whilst taking into account stochastic dependency between variables. These are typical characteristics for time and spatial correlation of forecast errors of demand and variable renewables. See [14]–[16] for the detailed theory and setup of copula-based MC simulations.

Typically, the dependency is provided in the form of a correlation matrix R . In real applications, this correlation matrix R could be built using updated meteorological data as shown in [15]. If the type of dependence is unknown and/or cannot be expressed by a correlation matrix due to a lack of adequate data, other methods could be used to generate appropriate samples, such as Vines [18] which do not require the full definition of the correlation matrix, or bounding approaches as developed in [20].

A pre-defined list of contingencies can be provided as another input. By applying the methodology to every item in the contingency list, contingency analysis is obtained.

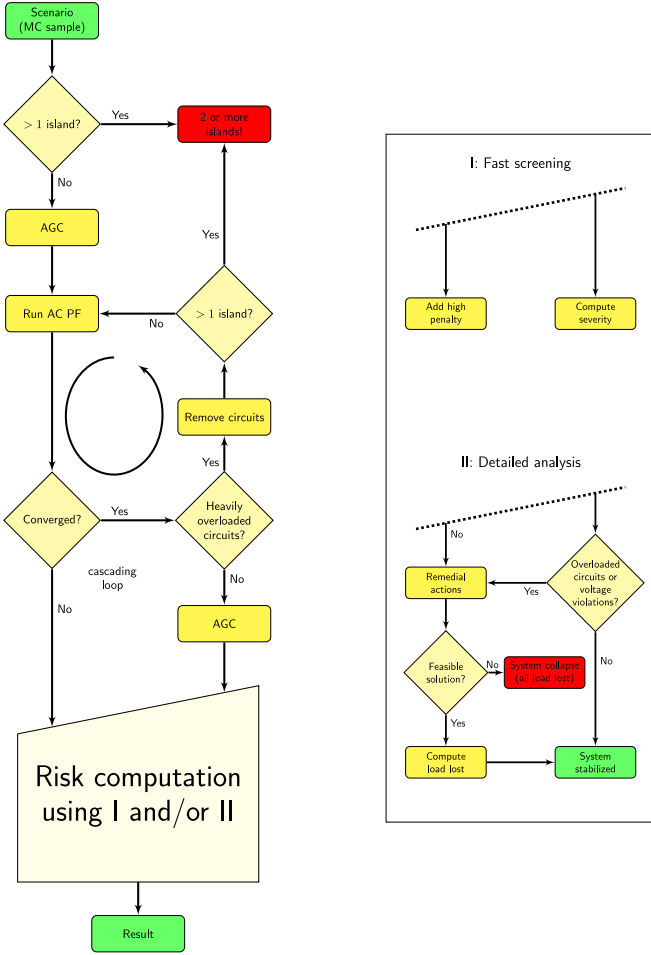


Fig. 2. Flowchart for 1 scenario (a single MC sample) (left) and two complementary tools to measure risk (right).

2) *Deterministic Security Assessment (DSA)*: For each sample of the MC simulation a detailed DSA model is used, see Fig. 2. The algorithm employs:

- 1) *Full AC computations*. Since voltage problems are often the generating causes of a system collapse, throughout the entire algorithm full AC computations are used². The algorithm employs a trust region AC PF solver, as a robust solver is paramount for the methodology. If, however, for a particular system state the AC PF does not converge, then it is assumed that this state is infeasible and a new set point needs to be determined. As an initial guess for each of the MC samples, a reference PF result is used rather than a flat start. This saves half of the number of iterations required for convergence of the AC PF.
- 2) *Cascading mechanism*. The model incorporates a mechanism to simulate cascading events. The mechanism is based on hard limits on the maximum allowable apparent power flowing through the circuits. This is similar to how cascading is modeled in [6].

²Approximate methods (e.g., methods based on DC computations) cannot adequately detect voltage problems which reduces their applicability in a realistic setup.

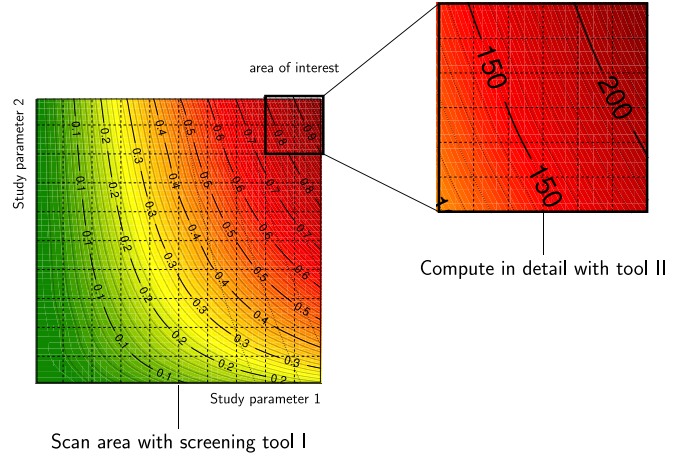


Fig. 3. The screening tool I and the detailed analysis tool II can work together to speed up the risk assessment. First, the system is screened with the fast tool I for interesting areas, typically risky system states. Next, the area of interest is computed thoroughly with the detailed analysis tool II.

- 3) *Automatic generation control (AGC)*. A model of zone-wise AGC is implemented to restore the power balance. Per zone the generators are adjusted by ratio to possible imbalances due to changes in demand.
- 4) *Islanding*. As a result of cascading, the power system may be divided into multiple sub systems, so-called islands. The algorithm verifies the existence of islanded networks and slack buses are added if required.
- 5) *Two risk measures*. The model integrates two risk measures, namely:
 - a) Tool I: a fast screening tool, which assesses the system risk quickly;
 - b) Tool II: a detailed analysis tool, which zooms in and defines remedial actions.

Since tool I is computationally cheap, hence fast, this tool may be used to screen the system for severe states. Thereafter tool II can be used to obtain more detailed information about these risky states. The additional information can be used to define actions for TSOs to steer the system into a risk-averse state. The concept of screening followed by a detailed analysis is shown in Fig. 3. The concept of severity functions is explained in more detail in Section II-B.

B. Tool I

Tool I is based on the concept of severity functions, see [6]. Two types of severity functions are used: i) for power flow through the circuits and ii) voltages at the buses. Here an implementation of linear severity functions is followed, as proposed in [7]. It is noticed that other severity functions, e.g., quadratic or exponential, can be implemented to increase the sensitivity of the algorithm to specific system areas.

- 1) *Severity Function for Overloaded Circuits*: Define a circuit's loading factor by

$$f = F_i / F_{i,\max},$$

where F_i is the actual apparent power flowing through circuit i and $F_{i,\max}$ its continuous rating. Here it is assumed that when

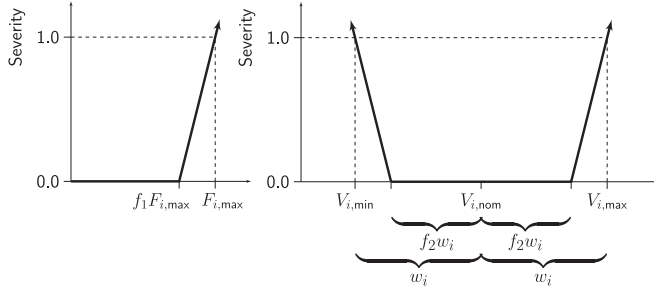


Fig. 4. Severity function for circuit overload (left) and severity function for too low and too high voltage (right).

the power through a circuit approaches its continuous rating ($f = 1$), this already jeopardizes the system's safety. A severity function for circuit overloading is defined accordingly as follows, see Fig. 4 (left).

The severity is defined to be zero up to $0 < f < f_1$, grows linearly above this threshold and for $f = 1.0$ the severity is exactly 1. Herein f_1 is a predefined value close to 1., e.g., $f_1 = 0.90$.

2) Severity Function for Too Low and Too High Voltage: Similarly, a severity function is defined for the voltage magnitudes V_i at each of the system buses. Suppose that the operating range for a bus i is $[V_{i,\min}, V_{i,\max}]$ [pu] with a nominal voltage right in between: $V_{i,\text{nom}} = (V_{i,\min} + V_{i,\max})/2$ [pu]. The width of the interval is $2w_i = (V_{i,\max} - V_{i,\min})$. Here it is assumed that when the voltage at a bus approaches its upper or lower limit, this starts to jeopardize the system's safety, see Fig. 4 (right). The truly safe operating range is set to be $[V_{i,\text{nom}} - f_2 w_i, V_{i,\text{nom}} + f_2 w_i]$, where f_2 is a predefined number close to 1, e.g., $f_2 = 0.90$. Outside this interval the severity grows linearly, and the severity is set to be exactly 1 when $V_i = V_{i,\min}$ and $V_i = V_{i,\max}$.

C. Tool II

Tool II provides a second risk indicator and is inspired by the work in [10].

1) Remedial Actions: The tool differentiates between four levels of risk:

- 1) No remedial actions are required; the system is already stable;
- 2) Manual re-dispatching of generator power is necessary to alleviate circuit overloading and/or voltage violations;
- 3) In addition to manual re-dispatching, load shedding is required to resolve the problems;
- 4) System collapse; the system cannot be stabilized anymore, the system is deemed to collapse.

A set of suitable remedial actions to alleviate severe system stress, i.e., voltage violations and circuits overloads, is proposed automatically. For this an AC OPF framework is used with the minimization of active re-dispatch as the objective function. Moreover, to make sure load shedding is used as a last resort, we added a high penalty for every MW of shedded load. In addition to the currently implemented remedial actions (re-dispatching

and load shedding), other ones, such as topology optimization, can readily be implemented within the AC OPF framework.

2) Risk Measure: Tool II differentiates between four levels of risk (see Section II-C1). Samples with risk levels 3 and 4 contribute to the expected amount of lost load, i.e.,

$$\mathbb{E}[\text{Lost Load}] = \frac{1}{N} \sum_{k=1}^N \text{lostload}_k,$$

where

$$\text{lostload}_k = \begin{cases} \sum_{b=1}^{N_B} (P_{B,b}^{\text{post}} - P_{B,b}^{\text{pre}}), & \text{risk level 3,} \\ \sum_{b=1}^{N_B} P_{B,b}^{\text{pre}}, & \text{risk level 4,} \end{cases} \quad (1)$$

is the amount of lost load for a sample k . In Equation (1) $P_{B,b}^{\text{post}}$ and $P_{B,b}^{\text{pre}}$ represent the amount of active load connected at a Bus b after and prior to load shedding, respectively. Similar formulas can be used for reactive load.

III. EXPERIMENTAL SETUP

In this section the experimental setup is discussed.

A. Implementation and Hardware

The presented methodology is implemented in MATLAB using the MATPOWER package [21] for power system modeling. The experiments are performed in parallel on a small cluster consisting of 6 nodes, each having a quad-core 3.5 GHz Intel i5-4690 processor and 32 GB DDR-3 RAM. The OS is Linux Debian 8.3 (64-bit) with kernel 4.2.6.

B. Test System

For the experiments the IEEE 118 bus test system is used. This test system consists of 118 buses, 54 generators and 186 circuits. Additional data is downloaded from http://motor.ece.iit.edu/data/JEAS_IEEE118.doc and is used to update MATPOWER's default 118 bus case file. Moreover, the following modifications are made in order to obtain an operational snapshot with increased cross-zonal flows:

- 1) The system is divided into three zones; Zone 1, Zone 2 and Zone 3, see Fig. 5;
- 2) The load in Zone 2 is increased to 150%;
- 3) The generation in Zone 2 is limited to 80% the original capacity and the generation in Zone 1 and Zone 3 is set to 110% the original capacity;
- 4) The continuous ratings of the transmission lines connecting Zone 1 and Zone 2 and the transmission lines connecting Zone 2 and Zone 3 are reduced to 70% of the original ratings.

The one-line representation of the test system is given in Fig. 5.

Due to the limited generation capacity in Zone 2, a great portion of the demand in Zone 2 is also served by generators from Zone 1 and Zone 3, leading to significant interface power flows (1 to 2 and 3 to 2). Moreover, the reduced capacity of the inter-zonal lines (indicated in red) leads to a higher system stress.

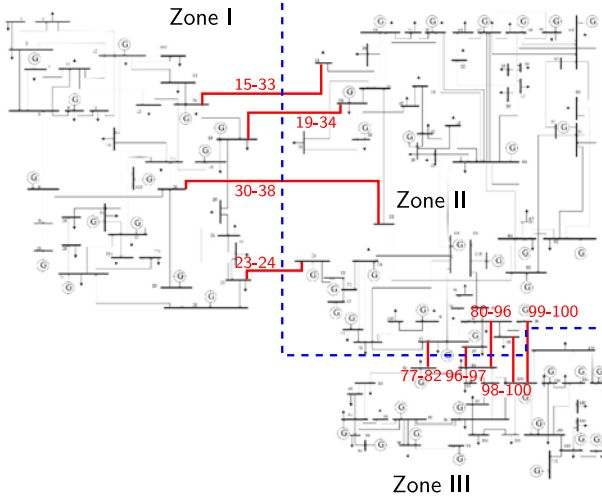


Fig. 5. The IEEE 118 bus test system, its division in three zones and interzonal transmission lines (red).

C. Stochastic Setup

In this paper snapshot data (point forecasts) are used to generate a PLF assuming normal distributions around the point forecasts and zone-wise uniform correlation. It is emphasized, however, that the methodology allows to work with other kind of distributions as well, such as beta or empirical distributions, depending on data availability. Also, the methodology can work with any correlation matrix R , and more complex relationships between active and reactive power.

This being remarked, the PLF based on snapshot data is generated as follows:

- 1) The fixed load (the point forecast) at each of the buses $1, 2, \dots, N_B$ is replaced by a normal distribution. These distributions indicate the load forecast uncertainty. Around the point forecasts a normal distribution is considered for the load forecast uncertainty, e.g., the active load at Bus b , denoted $P_{B,b}$, is given by

$$P_{B,b} \sim N(\mu_b, \sigma_b), \quad b = 1, 2, \dots, N_B, \quad (2)$$

where μ_b is the mean and σ_b is the standard deviation. The reactive load $Q_{B,b}$ at bus b is chosen such that $\tan \varphi = Q_{B,b}/P_{B,b}$ remains constant. For each of the MC samples, numbers are drawn from these active power distributions $P_{B,b}$. The reactive power sample $Q_{B,b}$ is computed accordingly. These $P-Q$ values indicate a specific realization of the respective forecast uncertainty.

- 2) In this paper zone-wise uniform³ correlation is considered. That is, for a power system having a total of N_B buses and being divided into n_z zones Z_1, Z_2, \dots, Z_{n_z} ,

$R \in \mathbb{R}^{N_B \times N_B}$ is given by:

$$R = \begin{bmatrix} R_1 & 0 & \cdots & 0 \\ 0 & R_2 & \cdots & 0 \\ \vdots & \vdots & \ddots & \vdots \\ 0 & 0 & \cdots & R_{n_z} \end{bmatrix},$$

where $R_z \in \mathbb{R}^{N_{B,z} \times N_{B,z}}$ is given by:

$$R_z = \begin{bmatrix} 1 & \rho_r & \cdots & \rho_r \\ \rho_r & 1 & \cdots & \rho_r \\ \vdots & \vdots & \ddots & \vdots \\ \rho_r & \rho_r & \cdots & \rho_r \end{bmatrix}, \quad z = 1, 2, \dots, n_z \quad (3)$$

and such that $\sum_z N_{B,z} = N_B$. In (3) the number ρ_r is the rank correlation.

- 3) Using the copula theory, MC samples are generated consistent to the marginal distributions and the correlation matrix R as follows:

- a) Correlated ranks $U_b (b = 1, \dots, N_B)$ are generated from standard uniform distributions using the Gaussian copula model and the provided correlation matrix R ;
- b) The correlated ranks U_b are transformed into marginal distributions by applying $F_{B,b}^{-1}$ to $U_b (b = 1, \dots, N_B)$.

In the above N_B is the number of system buses, and $F_{B,b}^{-1}$ are the inverse cumulative distribution functions of the active power distributions.

IV. CASE STUDY

In this study case a centrally dispatched⁴ system is analyzed in the presence of combined infeed forecast uncertainty (the system buses connect to distribution systems that contain loads and RES). The goal of this study is to show:

- 1) how Tool 1 and Tool II can work together;
- 2) the need for using an AC modeling framework;
- 3) the need for an advanced stochastic modeling;
- 4) the increase in computational speed by employing dynamic sampling methods.

The study is set-up and performed as follows:

- 1) An AC OPF with default cost functions is solved in order to compute the initial (safe) dispatch P^{pre} ;
- 2) No initial contingencies are considered; all lines and generators are online;
- 3) *Study parameter 1:* The forecast accuracy is increased gradually by increasing the standard deviation in the forecast error distributions: in (2) σ_b ranges from 0 to $0.05\mu_b$ in steps of 10%;
- 4) *Study parameter 2:* The rank correlation is increased gradually in order to investigate the impact to the estimation of

³Zone-wise uniform correlation allows for an easy understanding and it suffices to show that it is necessary to take into account stochastic dependence.

⁴In the central dispatch market system, the physical network and the market operation are strongly linked; technical constraints in the network are considered directly in the market clearing. The alternative is the self-scheduled market system in which the network is not considered directly in the market clearing [22].

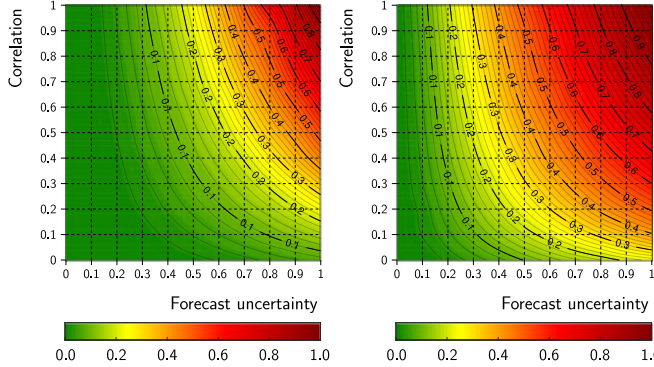


Fig. 6. Output Tool I: Normalized overload severity (left) and normalized voltage severity (right).

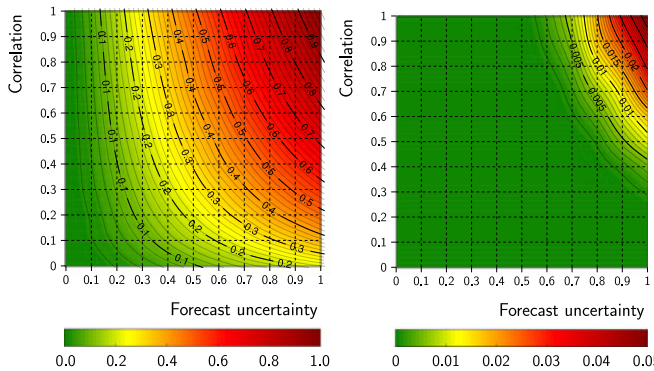


Fig. 7. Output Tool I: Normalized combined severity (left) and probability of cascading (right).

system risk when one uses methods that do not take correlation into account: in (3) ρ_r ranges from 0 (uncorrelated) to 1 (fully positively correlated) in steps of 10%.

The results are presented by means of iso-risk plots [6], with study parameter 1 on the x -axis and study parameter 2 on the y -axis.

A. Application of Tool I and Tool II

1) *Screening of the Domain With Tool I:* First the entire computational xy -domain is screened with Tool I to detect the most risky system states. In Fig. 6 the normalized overload severity (left) and the normalized voltage severity (right) is shown. In Fig. 7 the combined severity ($= 0.5 \cdot \text{voltage severity} + 0.5 \cdot \text{overload severity}$) and the probability of cascading is shown. The figures show that the highest risk is in the upper-right corner: the area with high forecast uncertainty and/or high correlation. The iso-risk plots were generated using 10.000 MC samples in every grid point, which took 14800 seconds (≈ 4 hours) on the small cluster.

2) *Detailed Analysis for Risky Region Using Tool II:* In the first step it was found that the highest risk is expected for system states corresponding to the upper-right corner of the domain. We decide to perform a detailed analysis with Tool II for this region. In Fig. 8 the lost active power is shown for this upper-right region consisting of 5×5 grid points. This iso-risk plot

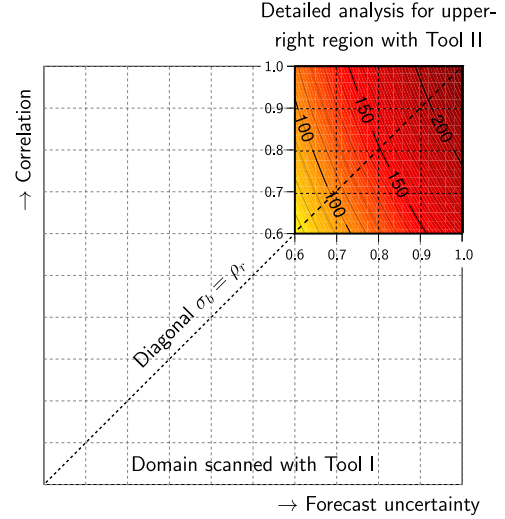


Fig. 8. A detailed analysis is performed for the (risky) upper-right region with Tool II. The numbers show the expected amount of lost active load in MW for this region.

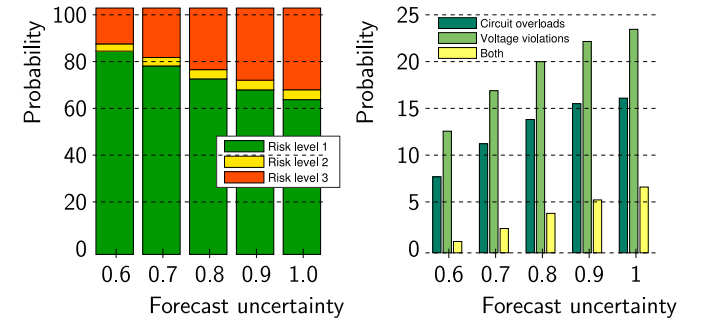


Fig. 9. Output Tool II: Risk levels (left) and risk causes (right) along the diagonal $\sigma_b = \rho_r$.

was generated using a fixed number of 10.000 MC samples in every grid point which took 25620 s (≈ 7 h) on the small cluster. A detailed analysis for the entire 11×11 -grid would have taken 54520 s (≈ 15 h). This shows how Tool I and Tool II should work together to speed up the risk assessment.

B. The Necessity of an Accurate AC Modeling

Tool II can provide various additional output. For example, in Fig. 9 (left) the risk is decomposed in the three key operational levels, see Section II-C1. In Fig. 9 (right) it is shown in how many cases circuit overloading, voltage violations or both caused the problems. In both graphs the risk is shown along the diagonal $\sigma_b = \rho_r$ (see Fig. 8).

The graph shows that although both circuit overload and voltage violations contribute to the system risk, voltage problems are more important. Methods that use DC approximations miss this important source of risk and AC methods are needed for the system security assessment.

C. The Need for an Advanced Stochastic Modeling

The study performed in Section IV-A shows the necessity of a detailed modeling of infeed stochasticity. As can be seen

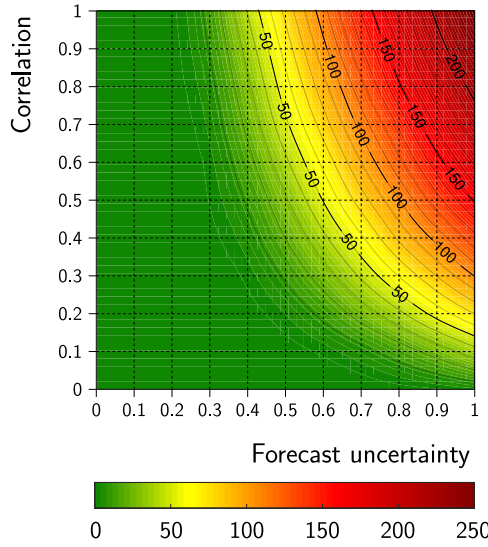


Fig. 10. Output Tool II: Lost active load in MW computed using dynamic sampling.

from Figs. 6–9, even if all other parameters stay unchanged, a severe underestimation of the system risk occurs if uncertainty (forecast accuracy) and/or correlation are not properly taken into account (points lying on the x - and/or y -axis). In practice this would mean that system operator would consider that the system is in a safe (green) mode, whereas in reality it may be in the risky (yellow/red) zone.

D. The Increase in Speed by Dynamic Sampling

The accuracy of the presented methodology depends on the volatility of the system inputs. This means that for efficiency the MC could be dynamic in the number of MC samples used. A dynamic number of MC samples yields a significant decrease in computational time without losing in accuracy.

To set-up an accuracy measure either of the different output quantities of Tools I and II can be used, e.g., overload severity (Tool I) or lost active load (Tool II). In this paper lost active load from Tool II is used and for the specific accuracy measure is taken the following. Let \bar{x} be the sample mean and s be the sample standard deviation of the lost load numbers. Then, the standard error $SE_{\bar{x},N}$ is defined to be:

$$SE_{\bar{x},N} = \frac{s}{\sqrt{N}}$$

where N is the sample size. The required number of MC samples N_{req} is defined to be:

$$N_{\text{req}} = \min \left\{ N : \frac{2SE_{\bar{x},N}}{\bar{x}} < \alpha \right\}, \quad (4)$$

where α is a predefined accuracy level, e.g., $\alpha = 0.05$ (5%). Moreover, in any case at least 10.000 MC samples are performed. If the average lost active load over these 10.000 samples is less than 1 MW, then the MC simulation can safely be aborted.

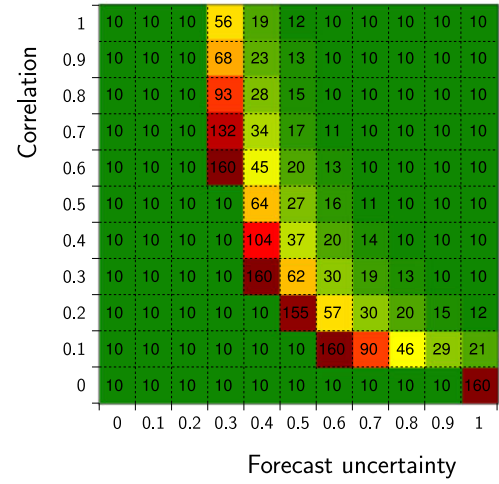


Fig. 11. Output Tool II: Required number of MC samples. The numbers in the cells show the required number of MC samples ($\times 1000$) in order to reach the predefined accuracy level of $\alpha = 0.05$ in this point.

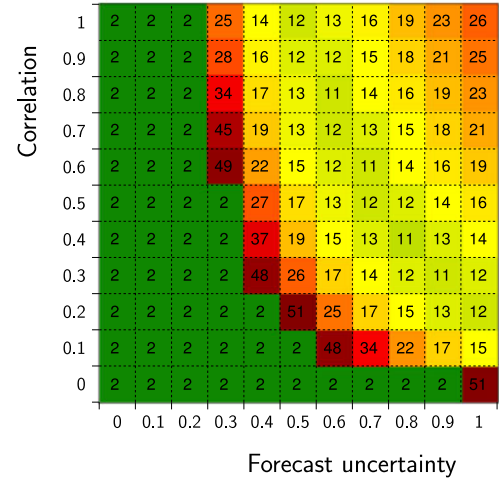


Fig. 12. Output Tool II: Required computation time in s. The numbers in the cells show the computation time in s ($\times 1000$) (right) in order to reach the predefined accuracy level of $\alpha = 0.05$ in this point.

In Fig. 10 the expected amount of lost load is computed with Tool II using dynamic sampling.

In Fig. 11 the required number of MC samples is shown in order to obtain the predefined accuracy measure (4) for the expected amount of lost load, and in Fig. 12 the corresponding computation time is shown.

In Fig. 11 the yellow-red band indicates the region of highest number of MC samples. The green areas indicate the regions of lowest number of MC samples. In the lower-left area the risk is virtually zero: the average lost load over 10.000 MC samples is less than 1 MW. In the upper-right area the risk is relatively large: in many MC samples load is shed and the standard error $SE_{\bar{x}}$ is relative small compared to the mean \bar{x} . Hence a relative small number of MC samples suffices to meet the accuracy measure (4). The yellow-red band indicates the region where lost load behaves a bit like a ‘rare event’, hence many MC

samples are required to reach the predefined accuracy. Note that this yellow-red band may be of particular interest to TSOs as it is the border between safe and risky operating states. Tool II can be used to determine whether a specific state in this band is considered to be safe or not.

If dynamic sampling was not used, then in every grid point 160.000 MC samples would have been used to obtain the predefined accuracy everywhere (in that case the most demanding case would define the sampling dimension). Hence a total of $11 \times 11 \times 160.000 = 19.4$ million samples. The total number of MC samples in our dynamic sampling is just 2.9 million, hence a reduction of $6.6 \times$.

In Fig. 12 the yellow-red region indicates the region of highest computation time. In contrast to the number of MC samples the upper-right corner is also yellow-red. This is due to the fact that in the upper-right corner the risk is high and hence many AC OPF problems are solved by Tool II. The total computation time for the entire iso-risk plot is 96.400 seconds (≈ 1.1 day). Again, if dynamic sampling was not used, then in every grid point 160.000 MC samples would have been used, resulting in a total computation time of 870.000 seconds (≈ 10 days). Hence the dynamic sampling gives an increase in speed of $9 \times$.

V. CONCLUSION

The presented methodology presents a setup for the incorporation of infeed uncertainty to the power system security assessment. The method combines a MC framework with a detailed DSA tool. The uncertainty analysis framework allows the incorporation of forecast uncertainty and correlation using copula functions. The DSA tool is based on an AC framework, utilizing a combination of risk metrics for maximum speed and accuracy: a screening tool based on severity functions that tracks the risk regions and a detailed tool based on AC OPF that can steer the system in risk-averse mode. The paper shows that using such a detailed framework for modeling the infeed uncertainty is key in order to properly assess system risk; any methodological compromises can lead to severe underestimation of system risk. Furthermore, an AC framework is needed, as voltage problems prove to have the highest contribution to the system risk. Finally, it was shown that the computations could be done within a reasonable amount of time. Tool I can be used to first detect the risky zones, whereafter Tool II is used for a thorough analysis of the risk zones. Dynamic sampling can be used to speed up the method as well by reducing the number of MC samples required to obtain a predefined level of accuracy. Furthermore, the methodology is easy to parallelize: (i) all grid points of the iso-risk plots can be computed fully in parallel, and (ii) per grid point the MC sampling can be done fully in parallel as well.

ACKNOWLEDGMENT

The authors would like to thank the partners from ETH Zürich and TU Graz for their feedback.

REFERENCES

- [1] G. Papaefthymiou and K. Dragoon, "Towards 100% renewable energy systems: Uncapping power system flexibility," *Energy Policy*, vol. 92, pp. 69–82, 2016.
- [2] D. Kirschen and D. Jayaweera, "Comparison of risk-based and deterministic security assessments," *IET Gener., Transm. Distrib.*, vol. 1, no. 4, pp. 527–533, 2007.
- [3] J. McCalley *et al.*, "Probabilistic security assessment for power system operations," in *Proc. IEEE Power Eng. Soc. General Meeting*, 2004, pp. 212–220.
- [4] J. McCalley, V. Vittal, and N. Abi-Samra, "An overview of risk based security assessment," in *Proc. IEEE Power Eng. Soc. Summer Meeting*, 1999, vol. 1, pp. 173–178.
- [5] UCTE, UCTE operation handbook—glossary, 2004. [Online]. Available: <https://www.entsoe.eu/publications/system-operations-reports/operation-handbook/>
- [6] M. Ni *et al.*, "Software implementation of online risk-based security assessment," *IEEE Trans. Power Syst.*, vol. 18, no. 3, pp. 1165–1172, Aug. 2003.
- [7] M. Ni, J. McCalley, V. Vittal, and T. Tayyib, "Online risk-based security assessment," *IEEE Trans. Power Syst.*, vol. 18, no. 1, pp. 258–265, Feb. 2003.
- [8] X. Li, X. Zhang, P. Lu, and S. Zhang, "Transmission line overload risk assessment for power systems with wind and load-power generation correlation," *IEEE Trans. Smart Grid*, vol. 6, no. 3, pp. 1233–1242, May 2015.
- [9] M. Marsadek and A. Mohamed, "Contingency screening using risk factor considering transmission line outage," *Int. J. Electr., Comput., Electron. Commun. Eng.*, vol. 9, no. 7, pp. 743–746, 2015.
- [10] D. Kirschen, D. Jayaweera, D. Nedic, and R. Allan, "A probabilistic indicator of system stress," *IEEE Trans. Power Syst.*, vol. 19, no. 3, pp. 1650–1657, Aug. 2004.
- [11] D. Kirschen, K. Bell, D. Nedic, D. Jayaweera, and R. Allan, "Computing the value of security," *IEE Proc.—Gener. Transm. Distrib.*, vol. 150, no. 6, pp. 673–678, 2003.
- [12] S. Hagspiel, A. Papaefthymiou, M. Schmid, and G. Andersson, "Copula-based modeling of stochastic wind power in europe and implications for the Swiss power grid," *Appl. Energy*, vol. 96, no. C, pp. 33–44, 2012.
- [13] M. de Jong, G. Papaefthymiou, D. Lahaye, C. Vuik, and L. van der Sluis, "Impact of correlated infeeds on risk-based power system security assessment," in *Proc. Power Syst. Comput. Conf.*, Wrocław, Poland, 2014, pp. 1–7.
- [14] G. Papaefthymiou, "Integration of stochastic generation in power systems," Ph.D. dissertation, Delft Univ. Technol., Delft, The Netherlands, 2006.
- [15] G. Papaefthymiou and P. Pinson, "Modeling of spatial dependence in wind power forecast uncertainty," in *Proc. 10th Int. Conf. Probab. Methods Appl. Power Syst.*, 2008, pp. 1–9.
- [16] G. Papaefthymiou and D. Kurowicka, "Using copulas for modeling stochastic dependence in power system security analysis," *Appl. Energy*, vol. 24, no. 1, pp. 40–49, 2009.
- [17] P. Embrechts, A. McNeil, and D. Straumann, "Correlation and dependence in risk management: properties and pitfalls," in *Risk Management: Value at Risk and Beyond*. Cambridge, U.K.: Cambridge Univ. Press, 1999, pp. 176–223.
- [18] D. Kurowicka and R. Cooke, *Uncertainty Analysis with High Dimensional Dependence Modelling* (Wiley Series in Probability and Statistics). New York, NY, USA: Wiley, 2006.
- [19] H. Louie, "Evaluation of bivariate archimedean and elliptical copulas to model wind power dependency structures," *Wind Energy*, vol. 17, pp. 225–240, 2014.
- [20] S. Ferson *et al.*, *Dependence in Probabilistic Modeling, Dempster-Shafer Theory, and Probability Bounds Analysis*. Albuquerque, NM, USA: Sandia Nat. Lab., 2003.
- [21] R. Zimmerman, C. Murillo-Sánchez, and R. Thomas, "Matpower: Steady-state operations, planning and analysis tools for power systems research and education," *IEEE Trans. Power Syst.*, vol. 26, no. 1, pp. 12–19, Feb. 2011.
- [22] L. Roald *et al.*, "Methods for optimization of power transits": Toolbox for Common Forecasting, Risk assessment, and Operational Optimization in Grid Security Cooperations of Transmission System Operators (TSOs)," ETH Zürich, Zürich, Switzerland, Tech. Rep. 48752-01, 2015.



Martijn de Jong received the M.Sc. degree in applied mathematics from Delft University of Technology, Delft, The Netherlands, in 2012.

He is currently a promovendus at Delft University of Technology, and did research for Work Package 4 of the FP-7 Umbrella project: the development of risk-based security assessment methods for power systems. His research interests include power system security analysis and the design of parallel iterative solvers on GPUs.



Georgios Papaefthymiou (M'03) received the Dipl.-Eng. degree in electrical and computer engineering from the University of Patras, Patras, Greece, in 1999, and the Ph.D. degree from Delft University of Technology, Delft, The Netherlands, in 2007.

He is currently with ELIA Grid International GmbH, Berlin, Germany, as a Senior Expert on power system operation and security, and with the Intelligent Electrical Power Grids group of Delft University of Technology as a Research Associate. His current research interests include power system flexibility,

modeling of uncertainty in power systems, and design of energy systems with large-scale penetration of distributed and stochastic generation.



Peter Palensky (M'03–SM'05) is a full Professor for intelligent electric power grids at Delft University of Technology, Delft, The Netherlands. Before that, he was Principal Scientist at the Austrian Institute of Technology, an Associate Professor at the Department of Electrical, Electronic and Computer Engineering, University of Pretoria, Pretoria, South Africa, a University Assistant at Vienna University of Technology, Vienna, Austria, and a Researcher at the Lawrence Berkeley National Laboratory, Berkeley, CA, USA. He is active in international committees like ISO, IEEE, and CEN. His main research interests include energy automation networks and modeling intelligent energy systems.